

# Identification of voltage-dependent $\text{Ca}^{2+}$ channels in sea urchin sperm

G. Granados-Gonzalez<sup>a</sup>, I. Mendoza-Lujambio<sup>a,b</sup>, E. Rodriguez<sup>a,c</sup>,  
B.E. Galindo<sup>a</sup>, C. Beltrán<sup>a</sup>, A. Darszon<sup>a,\*</sup>

<sup>a</sup> Department of Developmental Genetics and Molecular Physiology, Institute of Biotechnology, UNAM, Avenida Universidad 2001, Col. Chamilpa, CP 62210, Cuernavaca, Mor., Mexico

<sup>b</sup> National Medicine and Homeopathy School, IPN, Mexico City, Mexico

<sup>c</sup> Institute of Cell Physiology, UNAM, Mexico City, Mexico

Received 15 September 2005; revised 17 October 2005; accepted 18 October 2005

Available online 2 November 2005

Edited by Maurice Montal

**Abstract** Functional evidence indicates that voltage-dependent  $\text{Ca}^{2+}$  ( $\text{Ca}_v$ ) channels participate in sea urchin sperm motility and the acrosome reaction (AR), however, their molecular identity remains unknown. We have identified transcripts for two  $\text{Ca}^{2+}$  channel  $\alpha_1$  subunits in sea urchin testis similar in sequence to  $\text{Ca}_v1.2$  and  $\text{Ca}_v2.3$ . Antibodies against rat  $\text{Ca}_v1.2$  and  $\text{Ca}_v2.3$  channels differentially label proteins in the flagella and acrosome of mature sea urchin sperm. The  $\text{Ca}_v$  channel antagonists nifedipine and nimodipine, which inhibit the AR, diminish the intracellular  $\text{Ca}^{2+}$  elevation induced by a  $\text{K}^+$ -induced depolarization in valinomycin-treated sperm. These findings reveal that  $\text{Ca}_v1.2$  and  $\text{Ca}_v2.3$  channels could participate in motility and/or the AR in sea urchin sperm.

© 2005 Federation of European Biochemical Societies. Published by Elsevier B.V. All rights reserved.

**Keywords:** Speract; Calcium channels; Acrosome reaction; Motility

## 1. Introduction

Ionic flux regulates and controls sperm motility and the acrosome reaction (AR), two essential processes for fertilization in many species [1]. In sea urchins, the metabolic state and motility of sperm are modulated by small peptides called sperm-activating peptides (SAPs), which are released from the egg investments. These peptides facilitate gamete encounter and possibly the AR, acting in concert with other factors in the egg coat [2–4].

Speract, a 10 amino acid SAP from the egg jelly coat of *Strongylocentrotus purpuratus* and *Lytechinus pictus* [5,6], elicits a series of ion permeability changes which include a fast decrease in intracellular calcium concentration ( $[\text{Ca}^{2+}]_i$ ) [7] followed by a transient increase that involves at least two  $\text{Ca}^{2+}$  transport systems. The molecular identity of the transport mechanisms underlying these multi-phasic  $[\text{Ca}^{2+}]_i$  changes is unknown, but they possibly include voltage-dependent  $\text{Ca}^{2+}$

( $\text{Ca}_v$ ) channels and  $\text{Ca}^{2+}$  transporters [7–12]. Furthermore, the AR, an exocytotic reaction necessary for sperm to fuse with the egg, is also dependent on regulated changes in  $[\text{Ca}^{2+}]_i$ . During this reaction, the acrosome vesicle on the tip of the sea urchin sperm head fuses with the plasma membrane. The egg-coat component that induces the AR is a fucose sulfated glycoconjugate (FSG) [13]. Upon its binding to the sperm, FSG transiently opens a  $\text{Ca}^{2+}$ -selective channel that is blocked by the  $\text{Ca}_v$  channel inhibitors verapamil and dihydropyridines [14]. Seconds later, a second channel, possibly a store-operated  $\text{Ca}^{2+}$  channel insensitive to the latter blockers, activates and leads to vesicular fusion [15,16].

Because certain  $[\text{Ca}^{2+}]_i$  changes triggered by speract [7,11] and FSG [16,17] are influenced by dihydropyridines and other  $\text{Ca}_v$  channel blockers, it has been proposed that  $\text{Ca}_v$  channels participate in these sperm processes. However, to date no  $\text{Ca}_v$  channel from sea urchin sperm has been unequivocally identified. Only two sea urchin sperm ion channels have been cloned and both are hyperpolarization and cyclic nucleotide gated channels, SpHCN1 [18] and SpHCN2 [19].

The major function of  $\text{Ca}_v$  channels is to convert membrane potential changes into intracellular  $\text{Ca}^{2+}$  signals. The  $\text{Ca}_v$  channel permeation pathway is formed by its  $\alpha_1$  subunit, which is encoded by a family of at least 10 genes in mammals. Each  $\alpha_1$  subunit is composed of four repeated domains (I–IV), each containing six transmembrane alpha helices (S1–S6) surrounding a central pore [20,21].  $\text{Ca}_v$  channels fall into two major functional classes: high voltage-activated (HVA) and low voltage-activated (LVA) channels. HVA channels open following strong depolarizations and have been classified according to the biophysical and pharmacological characteristics of their currents into L-, N-, P/Q- and R-type. This class of channels is encoded by 7 members of the  $\alpha_1$  family:  $\text{Ca}_v1.1$  to 1.4 and  $\text{Ca}_v2.1$  to 2.3 [20,21]. The current through HVA channels may be modulated by alternative splicing of the  $\alpha_1$  subunit mRNA, by the presence of auxiliary subunits ( $\beta$ ,  $\gamma$  and  $\delta$ ) and by post-translational modifications [20,22]. LVA  $\text{Ca}_v$  channels, also known as T-type, include  $\text{Ca}_v3.1$  to 3.3.

The known invertebrate  $\text{Ca}_v$  channels may be classified into similar  $\text{Ca}_v$  subclasses as in mammals, based on pharmacological sensitivities to organic and inorganic antagonists and channel kinetics [23]. Cloning of  $\text{Ca}^{2+}$  channel subunits from various invertebrate species has helped to clarify the organization and evolution of metazoan  $\text{Ca}^{2+}$  channel genes [24].

The present report describes for the first time the presence of two  $\text{Ca}^{2+}$  channel  $\alpha_1$  subunits related to the mammalian HVA

\*Corresponding author. Fax: +52 777 317 2388.

E-mail address: [darszon@ibt.unam.mx](mailto:darszon@ibt.unam.mx) (A. Darszon).

**Abbreviations:** ASW, artificial sea water;  $[\text{Ca}^{2+}]_i$ , intracellular calcium concentration; AR, acrosome reaction;  $\text{Ca}_v$ , voltage-dependent  $\text{Ca}^{2+}$ ; SAP, sperm-activating peptide; HVA, high voltage-activated; LVA, low voltage-activated

Ca<sub>v</sub>1.2 and Ca<sub>v</sub>2.3 in sea urchin testes. These transcripts were detected by Northern blot and RT PCR. Mammalian antibodies to these two Ca<sup>2+</sup> channel  $\alpha_1$  subunits differentially recognized proteins along mature sea urchin sperm. Nifedipine and nimodipine, which influence motility and/or inhibit the AR, diminish the [Ca<sup>2+</sup>]<sub>i</sub> increase induced by a K<sup>+</sup>-induced depolarization in valinomycin-treated sperm, corroborating the presence of Ca<sub>v</sub> channels in these cells.

## 2. Materials and methods

### 2.1. Gametes and reagents

*Strongylocentrotus purpuratus* and *Lytechinus pictus* sea urchins were obtained from Marinus (Long Beach, CA, USA) and from Pamanes Inc. (Ensenada, Baja California, Mexico). Spawning was induced by an intracoelomic injection of 0.5 M KCl. Dry sperm were collected and kept on ice until used. Artificial seawater (ASW) contained (mM): 450 NaCl, 10 KCl, 10 CaCl<sub>2</sub>, 26 MgCl<sub>2</sub>, 30 MgSO<sub>4</sub>, 2.5 NaHCO<sub>3</sub>, 10 HEPES, 0.1 EDTA (pH 8.0, 950–1000 mOsm). Low Ca<sup>2+</sup> ASW pH 7.0 = ASW at pH 7.0 but with 1 mM instead of 10 mM CaCl<sub>2</sub>. Nimodipine was from Tocris Cookson Inc. Nifedipine was from Sigma–Aldrich. 2-(2-(4-Nitrobenzyloxy) phenyl) isothiurea methanesulphonate (KB-R7943) was a gift from Dr. Vacquier (University of California, San Diego, CA, USA). Antibodies anti-Ca<sub>v</sub>2.1, 2.2, 2.3, 2.4; anti-Ca<sub>v</sub>1.2, 1.3; anti-Ca<sub>v</sub>3.1, 3.3 and anti-Pan were from Alomone Labs (Jerusalem Israel). Alexa 488, Alexa 594 and Fluor4-AM were from Molecular Probes Inc. (Eugene, OR, USA). The rest of the reagents were of the highest quality available.

### 2.2. RT PCR experiments and cloning

RNA from *S. purpuratus* testes was extracted using TRIzol Reagent (Sigma) according to the manufacturer's instructions. cDNA was synthesized from total RNA by random hexamer-primer reverse transcription (Superscript II RNase H-Reverse transcriptase, Invitrogen). cDNA was then subjected to PCR amplification using Titanium Taq DNA Polymerase (Clontech). The primers used to amplify PCR fragments for the Ca<sub>v</sub>1.2 and Ca<sub>v</sub>2.3 (A1C forward: 5'-ATG CTG ACC GTG TTC CA-3', A1C reverse: 5'-ATC CTC CTC TAT CTG TTG CTT-3'; A1Eb forward: 5'-GCC CAG CAG ACA CCT AAC-3', A1Eb reverse: 5'-AAC ACG CAG TCA AAC ACG-3') were designed using as template those sequences from the sea urchin genome database (<http://www.hgsc.bcm.tmc.edu/projects/seaurchin/>) that aligned with rat Ca<sub>v</sub>1.2 and 2.3 sequences.

### 2.3. Sequence analysis

Amplified products were sequenced and blasted (tBLASTx) against the non-redundant GenBank database (<http://www.ncbi.nlm.nih.gov/BLAST/>) in order to confirm their identity. The cDNA sequences were translated into the corresponding peptide sequences, and then analyzed by means of several computational bioinformatics tools: CLUSTALW in the BioEdit program was used for alignments; transmembrane regions and domains were predicted with SMART (<http://smart.embl-heidelberg.de/>) and TMHMM (<http://www.cbs.dtu.dk/services/TMHMM-2.0/>) programs.

### 2.4. Phylogenetic analysis

Complete sequences from various organisms were used to generate a neighbor-joining phylogenetic tree (Fig. 2) of Ca<sub>v</sub> channels. Ca<sub>v</sub>3.1 from human was used as outgroup. The tree was made using the program MEGA3 [25] with 3000 replications and Poisson correction. GenBank Accession Nos. were: Q13698, human Ca<sub>v</sub>1.1; O57483, frog Ca<sub>v</sub>1.1; P22316, carp Ca<sub>v</sub>1.1; NP\_000710, human Ca<sub>v</sub>1.2; Q01815, mouse Ca<sub>v</sub>1.2; NP\_571975, zebrafish Ca<sub>v</sub>1.2; NP\_000711, human Ca<sub>v</sub>1.3; AAS20586, zebrafish Ca<sub>v</sub>1; P27732, rat Ca<sub>v</sub>1.3; NP\_005174, human Ca<sub>v</sub>1.4; NP\_062528, mouse Ca<sub>v</sub>1.4; NP\_000059, human Ca<sub>v</sub>2.1; NP\_037050, rat Ca<sub>v</sub>2.1; CAI11858, zebrafish Ca<sub>v</sub>2.1; NP\_000709, human Ca<sub>v</sub>2.2; NP\_671482, rat Ca<sub>v</sub>2.2; P56698, electric ray Ca<sub>v</sub>2.2; NP\_000712, human Ca<sub>v</sub>2.3; Q07652, rat Ca<sub>v</sub>2.3; P56699, electric ray Ca<sub>v</sub>2.3; AAD11470, coral; AAC63050, jelly fish; BAA13136 squid and BAA34927, ascidian. The Ca<sub>v</sub> channel cDNA

fragments access numbers are: DQ185022 for suCa<sub>v</sub>L and DQ185022 for suCa<sub>v</sub>NL. The predicted sea urchin Ca<sub>v</sub> sequences are: XP\_780220 for suCa<sub>v</sub>NL and XP\_783410 for suCa<sub>v</sub>L.

### 2.5. Immunolocalization

Sea urchin sperm were diluted (1:900) in ASW and the coelomocytes were removed. Sperm were bound onto glass slides coated with a bio-adhesive (Electron Microscopy Sciences, Ft. Washington, PA, USA) and allowed to settle for 60 min. Samples were immediately fixed with 4% paraformaldehyde in ASW pH 8.0 for 10 min, rinsed with PBS (3 times, 5 min), permeabilized with 0.1% Triton X-100 for 10 min, and blocked with 2% BSA for 1–2 h. Thereafter, samples were incubated overnight at 4 °C in a 1:50 dilution of primary antibodies and 2% BSA-PBS. After rinsing with PBS (3 times, 5 min), samples were incubated 1 h at RT with Alexa Fluor 594 or 488 goat anti-rabbit IgG, and rinsed again with PBS (3 times, 5 min) before they were examined with a confocal laser-scanning microscope (BioRad 600, Zeiss LSM 510 Meta). Control experiments were performed by pre-incubation of the primary antibodies with their respective antigenic peptides. Images shown are representative of at least three separate experiments under each condition.

### 2.6. Western immunoblotting

Sperm plasma membranes were isolated as in Garcia-Soto et al. [26]. They were dissolved in loading buffer and subjected to SDS-PAGE and Western blotting. Ca<sub>v</sub> antibodies anti-Ca<sub>v</sub>1.2, anti-Ca<sub>v</sub>2.3 and anti-Pan were diluted 1:200. Control experiments were performed incubating the primary antibody with a fivefold excess of the antigenic peptide. Signals were detected with the ECL system (Amersham).

### 2.7. [Ca<sup>2+</sup>]<sub>i</sub> measurements

Sperm population [Ca<sup>2+</sup>]<sub>i</sub> measurements were performed on a SLM 8000 Aminco spectrofluorometer with a temperature-controlled cell holder equipped with a magnetic stirrer, at 16 °C. Sea urchin sperm were loaded with Fluo-4 (excitation 505 nm and emission 525 nm) as previously reported [27]. 10  $\mu$ l of the sperm suspension were added to a round cuvette containing 1.6 ml ASW, pH 8.0 at 16 °C. The suspension was stirred constantly and left to equilibrate for 1 min before proceeding to the assay.

## 3. Results

### 3.1. Sequence analysis

Transcripts from both Ca<sub>v</sub> L-type and Ca<sub>v</sub> non-L-type could be amplified by RT PCR using *S. purpuratus* testes cDNA (Fig. 1A). The sequenced transcripts were blasted (tBLASTx) against the non-redundant database at NCBI and both have a high similarity with Ca<sub>v</sub> channels. One fragment, corresponding to Ca<sub>v</sub> L-type channels and named suCa<sub>v</sub>L, had the expected length (243 bp) and encodes a fragment of 81 amino acids (aa) that shows 78% identity with a 81 aa fragment (aa 354–434) from rat Ca<sub>v</sub>1.2 (NP\_058994) (Fig. 1B). The other non-L-type fragment, named suCa<sub>v</sub>NL, is 651 bp long and is shorter than the corresponding fragment in rat Cav2.3 (1580 bp), NP\_037050. However, the translated sequence has a high similarity with rat Ca<sub>v</sub>2.3 in two segments flanking the amplified region (similarity of 59% and 74%, respectively) (Fig. 1C). suCa<sub>v</sub>L shows the highest similarity (92%) with human Ca<sub>v</sub> L-type (A45290) and suCa<sub>v</sub>NL (57%) with Ca<sub>v</sub> non-L-type from snail AAO83841 (not shown).

Fragment suCa<sub>v</sub>L corresponds to the S6 of domain I from rat Ca<sub>v</sub>1.2 and fragment suCa<sub>v</sub>NL to the S1, S2 and S3 of domain II from rat Ca<sub>v</sub>2.3 (Fig. 1). With the use of the contigs from the sea urchin genome database, we predicted partial sequences for suCa<sub>v</sub>L and suCa<sub>v</sub>NL (data not shown). While the paper was in revision, the first annotation of the Sea Urchin Genome Project appeared at the NCBI site and we used our

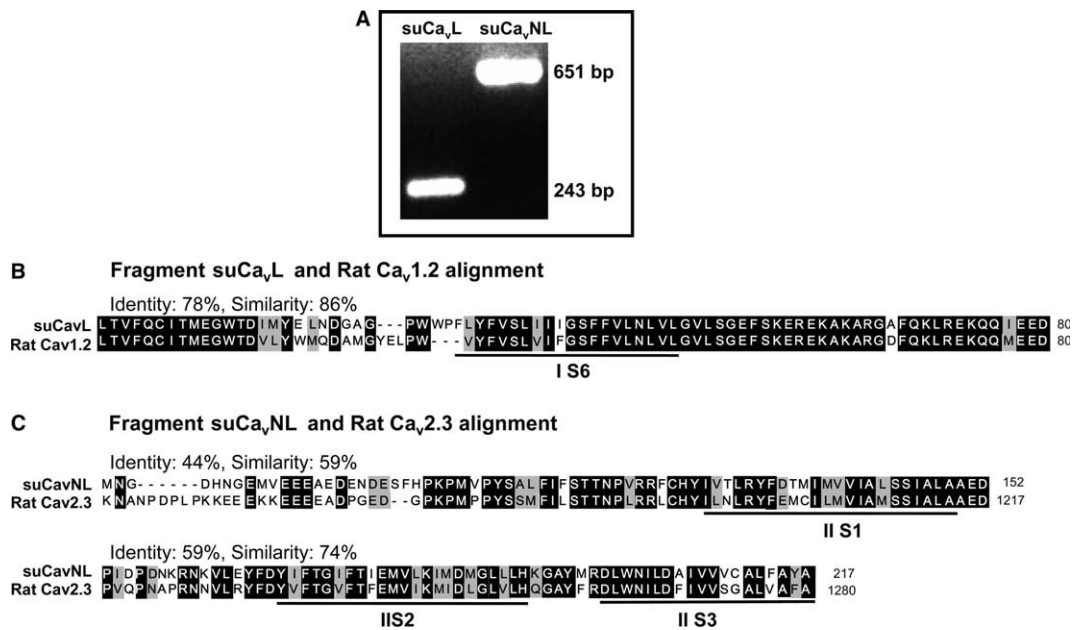


Fig. 1. suCa<sub>v</sub>L and suCa<sub>v</sub>NL are expressed in *S. purpuratus* sperm. (A) RT PCR using *S. purpuratus* testes cDNA. The amplified fragment for suCa<sub>v</sub>L is 243 bp long and the fragment for suCa<sub>v</sub>NL is 651 bp long. Their identity was confirmed by sequencing as L-type and non-L-type Ca<sub>v</sub> channels, respectively. (B) Alignment of suCa<sub>v</sub>L and rat Cav1.2, the transmembrane segment IS6 is underlined. This alignment gives a residue identity of 78%. (C) Alignment of suCa<sub>v</sub>NL and rat Ca<sub>v</sub>2.3, transmembrane regions IIS1, IIS2 and IIS3 are underlined. In this case, the amino acid sequence of suCa<sub>v</sub>NL aligns with the flanking regions of the intended region to be amplified; then, there are 352 residues in between. The sequence corresponding to the 5' flanking region (rat Ca<sub>v</sub>2.3, 1–778aa) is 44% identical and the 3' region (rat Ca<sub>v</sub>2.3, 1139–1280aa) has an identity of 59%. Black shaded amino acids are identical, grey shaded residues are similar according to matrix BLOSUM 62. Percentage of similarity and identity is shown for each alignment.

partial sequences to pull out the predicted sequences. This information will now make it easier to obtain the complete clones of these two channels in order to do functional assays by heterologous expression.

### 3.2. Phylogenetic analysis

The neighbor-joining phylogenetic tree originated with representative Ca<sub>v</sub> channel sequences (Fig. 2) shows that the suCa<sub>v</sub>L fragment falls into the L-type family and the suCa<sub>v</sub>NL is member of the non-L-type Ca<sub>v</sub> family. In addition, using the predicted sequences instead of the fragments, the topology of the tree remains identical (Fig. 2). These sea urchin Ca<sub>v</sub> channels do not belong to any of the groups already conformed by mammals, they seem to belong to different subgroups which diverged earlier than their mammal partners did.

### 3.3. suCa<sub>v</sub>s expression is detected in *S. purpuratus* testes

Northern blot analysis with total RNA from *S. purpuratus* testes from both suCa<sub>v</sub>s was performed. Two bands of around 7.0 and 3.2 Kb were obtained for suCa<sub>v</sub>L. The 7.0 Kb band is consistent with the length from most L-type Ca<sub>v</sub>s. With suCa<sub>v</sub>NL, we obtained three bands of around 6.0, 3.2 and 1.5 Kb; the 6.0 Kb band is consistent with the length from most non-L-type Ca<sub>v</sub>s (not shown).

### 3.4. Protein analysis of suCa<sub>v</sub>L and suCa<sub>v</sub>NL in *S. purpuratus* and *L. pictus* sperm

The high homology of suCa<sub>v</sub>L with rat L-type Ca<sub>v</sub>1.2 and suCa<sub>v</sub>NL with rat non-L-type Ca<sub>v</sub>2.3 encouraged us to test the commercially available rat antibodies against different Ca<sub>v</sub> channels, by immunolocalization and Western blot in sea urchin sperm. The set of antibodies included a general anti-

body that detects a domain present in all HVA Ca<sub>v</sub> channels (anti-Pan). Immunofluorescence was detected in sea urchin sperm flagella, acrosomes and mitochondria with anti-Ca<sub>v</sub>1.2, Ca<sub>v</sub>2.3 and Pan antibodies (Fig. 3). Anti-Pan stained the base of the head where the mitochondrion is located, the acrosome (fluorescent dot) and the flagella with a weak and punctuated fluorescent pattern. Ca<sub>v</sub>1.2 staining was more pronounced and evenly distributed in the tail, and almost imperceptible in the tail-head connection. In contrast, Ca<sub>v</sub>2.3 displayed a very strong signal in the mitochondrial area and an intense fluorescent dot in the acrosome. Flagellar labelling with this antibody was sparse. The discrete staining patterns revealed by the different Ca<sub>v</sub> α1 subunit antibodies in sea urchin sperm suggest the expressed channels may be separately involved in different functions such as motility and the AR.

The antibodies employed were raised against rat Ca<sub>v</sub> channels. To test their specificity in sea urchin sperm we performed immunolocalization controls by incubating the antibodies with their corresponding antigenic peptide for anti-Ca<sub>v</sub>1.2, anti-Ca<sub>v</sub>2.3 and anti-Pan. Under these conditions none of the three antibodies gave a signal (not shown), confirming their specificity. Furthermore, antigenic peptides from Ca<sub>v</sub>2.1, Ca<sub>v</sub>2.3, Ca<sub>v</sub>3.1 and TRPC6 could not block labelling by anti-Ca<sub>v</sub>1.2 or Ca<sub>v</sub>2.3 (except its corresponding peptide), thus, demonstrating the specificity of their inhibitory action. We then searched for the sequences of the corresponding antigenic peptides within the partial and the predicted sequences for suCa<sub>v</sub>L1 and suCa<sub>v</sub>NL1 we had found. The only antigenic peptide present in both suCa<sub>v</sub>s sequences was that of anti-Pan, which corroborates the presence of Ca<sub>v</sub> channels in sea urchin sperm. We cannot conclude that the other peptide sequences are absent, as the suCa<sub>v</sub> sequences are predicted but not confirmed and the cDNA sequences we found are still incomplete.

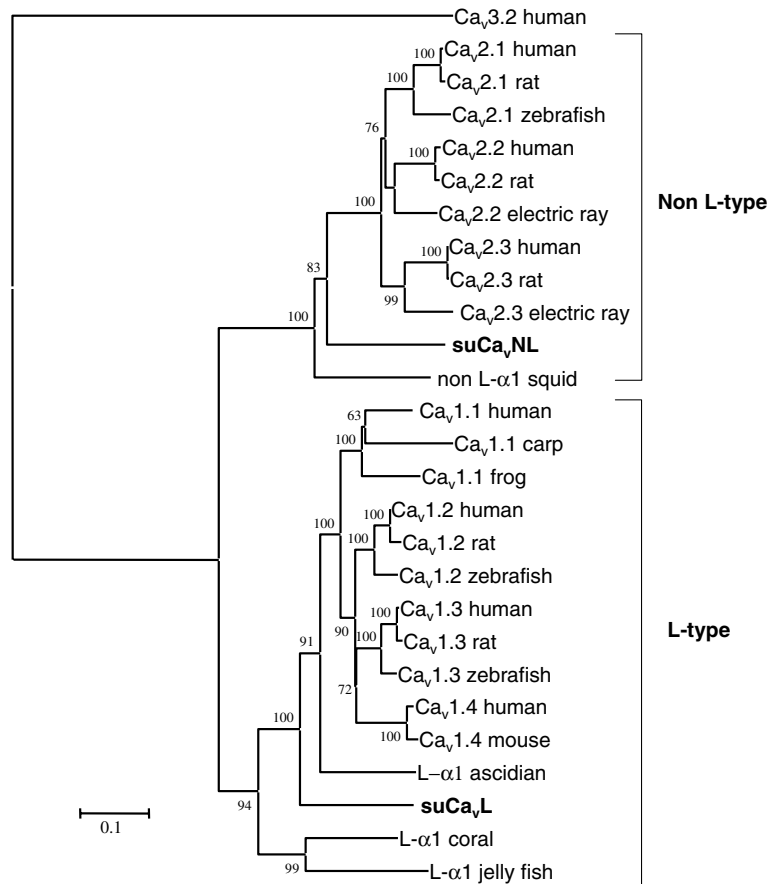


Fig. 2. Phylogenetic analysis of  $\text{Ca}^{2+}$  channel  $\alpha 1$  subunits. Neighbor-joining tree made with the alignment of 26 full length sequences from different species.  $\text{Ca}_v3.2$  from human was used as out group. The two sea urchin sequences are in bold. Numbers at interior nodes are bootstrap percentages from 3000 replications. Accession numbers for sequences are enlisted in Section 2.

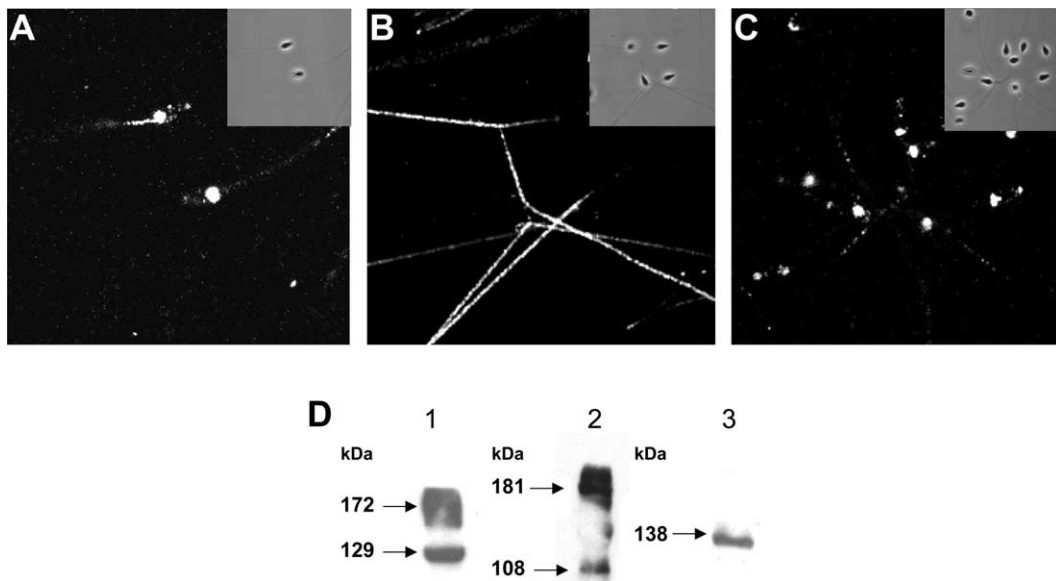


Fig. 3.  $\text{Ca}_v$  channels immunolocalization in sea urchin sperm. Representative confocal micrograph sperm stained with Pan (A),  $\text{Ca}_v1.2$  (B) and  $\text{Ca}_v2.3$  (C) specific antibodies showing the immunofluorescence localization of the proteins. Inset represents the corresponding phase contrast images. (D) Western blots demonstrating the expression of  $\text{Ca}_v$  proteins in sea urchin sperm, sperm flagellar membranes blotted with anti-Pan (1), anti- $\text{Ca}_v1.2$  (2) and anti- $\text{Ca}_v2.3$  (3) specific antibodies.

To further test the specificity of the  $\text{Ca}_v$  antibodies, Western blot analyses were performed with sea urchin flagellar membranes. The results are consistent with our immunofluorescence findings. All antibodies mentioned above (Section 2) were tested, but bands were only obtained with anti- $\text{Ca}_v1.2$ , anti- $\text{Ca}_v2.3$  and anti-Pan. Anti- $\text{Ca}_v1.2$  revealed two bands of approximately 181 and 108 kDa (Fig. 3D2). Anti- $\text{Ca}_v2.3$  stained one band of about 138 kDa (Fig. 3D3). Using anti-Pan, we observed two bands of 172 and 129 kDa (Fig. 3D1). All the bands detected, several of which are reported by the  $\text{Ca}_v$  antibody supplier, were completely blocked when the antibodies were incubated with their corresponding antigenic peptides (PEP). As before, the antigenic peptides from the other  $\text{Ca}_v$  channels could not compete with anti- $\text{Ca}_v1.2$  staining. It is worth noting that similar results (not shown) were obtained when the  $\text{Ca}_v$  antibodies were tested in *L. pictus* sperm.

### 3.5. $\text{Ca}_v$ channels are functionally present in sea urchin sperm

To investigate whether the  $\text{Ca}_v$  channels reported by the antibodies are functional in sea urchin sperm, we measured  $[\text{Ca}^{2+}]_i$  increases in sperm populations following depolarization in the presence and absence of dihydropyridines. These experiments were performed with *L. pictus* sperm, in which the  $\text{Ca}_v$  channel antibody staining patterns are very similar to those we report in *S. purpuratus* sperm (not shown). *L. pictus* sperm were hyperpolarized with 1  $\mu\text{M}$  valinomycin in

1 mM KCl ASW to remove  $\text{Ca}_v$  channel voltage-dependent inactivation [28]. Thereafter, the cells were depolarized by increasing external  $\text{K}^+$  to 20 mM. Fig. 4A illustrates the increase in  $[\text{Ca}^{2+}]_i$  induced by the  $\text{K}^+$  addition. Treatment with the  $\text{Ca}_v$  channel antagonists nifedipine (30  $\mu\text{M}$ ) or nimodipine (30  $\mu\text{M}$ ) inhibited 20–30% of the control  $[\text{Ca}^{2+}]_i$  increase. 20  $\mu\text{M}$  of KB-R7943, a  $\text{Na}^+/\text{Ca}^{2+}$  exchanger inhibitor, did not affect  $[\text{Ca}^{2+}]_i$ . Fig. 4B presents a summary of the results.

## 4. Discussion

Functional studies have implicated the participation of  $\text{Ca}^{2+}$  channels in sea urchin sperm physiology [1,16,17]. However, the identity of the  $\text{Ca}^{2+}$  channels in sea urchin sperm has not previously been established.  $\text{Ca}_v$  channel antagonists inhibit the AR induced by the egg investments and influence the sperm-induced changes in  $[\text{Ca}^{2+}]_i$ , membrane potential and motility, indicating a relevant role for these channels in these important sperm functions [7,9,11,14,16,29,30]. Furthermore,  $\text{Ca}_v$  channel subunits are present in mature mammalian sperm [31–35] and in many invertebrate species [24].

The *S. purpuratus*  $\text{Ca}_v$  channels have the general structural characteristics of the members of the  $\text{Ca}_v$  channel superfamily. Even though the sequences of  $\text{suCa}_v\text{L}$  and  $\text{suCa}_v\text{NL}$  are partial, they contain a section of the domains I and II, respectively, and  $\text{suCa}_v\text{NL}$  has one of the conserved EEEE motif required for  $\text{Ca}^{2+}$  selectivity of  $\text{Ca}_v$  channels [36]. It was thus not entirely unexpected that the antibodies against  $\text{Ca}_v$  channels generated from rat sequences could detect these proteins in the sea urchin sperm.

Consistent with the findings above described, we found in *S. purpuratus* testis one partial cDNA sequence for a  $\text{Ca}_v \alpha 1$  subunit ( $\text{suCa}_v\text{L}$ ) that shares homology with L-type channels, and another sequence that is similar to non-L-type  $\text{Ca}_v$  channels ( $\text{suCa}_v\text{NL}$ ).

Furthermore, using all the commercially available antibodies to mammalian  $\text{Ca}_v$  channels, we detected by immunocytochemistry as well as by Western blot, signals in sperm with anti- $\text{Ca}_v1.2$  and anti- $\text{Ca}_v2.3$ , and as anticipated with anti-Pan.  $\text{Ca}_v1.2$  and  $\text{Ca}_v2.3$  have previously been detected in mouse [37] and human sperm [34].

Functional studies using  $\text{Ca}_v$  channels blockers in sea urchin sperm indicate that  $\text{Ca}_v$  channels participate in motility and/or the AR. Since the identified  $\text{Ca}_v$  channels  $\text{suCa}_v\text{L}$  and  $\text{suCa}_v\text{NL}$  are present in the sperm head and flagella of this species, we suggest that they may play an important role in motility and/or the AR.

**Acknowledgments:** We thank Xochitl Alvarado and Andres Saralegui for confocal imaging, Jorge Yáñez for DNA sequencing and Eugenio López for primer synthesis and Dr. Chris Wood for reading the manuscript. Supported by CONACyT and DGAPA-UNAM to G.G., A.D. and C.B. and FIRCA RO3 TW 00612 and the Wellcome Trust to A.D.

## References

- [1] Darszon, A., Beltran, C., Felix, R., Nishigaki, T. and Trevino, C.L. (2001) Ion transport in sperm signaling. *Dev. Biol.* 240, 1–14.
- [2] Morisawa, M. (1994) Cell signaling mechanisms for sperm motility. *Zool. Sci.* 11, 647–662.

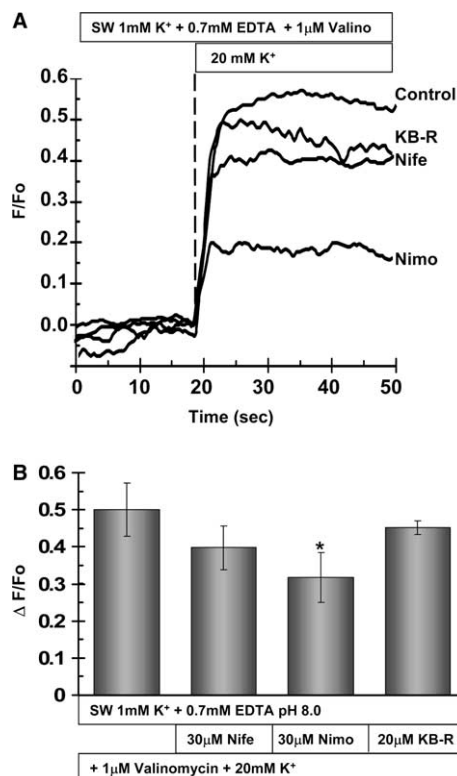


Fig. 4. Intracellular  $\text{Ca}^{2+}$  experiments show the functional presence of  $\text{Ca}_v$  channels in sea urchin sperm. Sperm loaded with Fluo-4 (see Section 2) were suspended in SW 1 mM  $\text{K}^+$  0.7 mM EDTA plus 1  $\mu\text{M}$  valinomycin to hyperpolarize sperm and remove  $\text{Ca}_v$  channels inactivation.  $\text{Ca}^{2+}$  channel opening was evaluated by 20 mM  $\text{K}^+$  addition to depolarize membrane potential in presence of 30  $\mu\text{M}$  Nifedipine, 30  $\mu\text{M}$  nimodipine and 20  $\mu\text{M}$  KB-R7943 (A). The bars represent the means  $\pm$  S.E.M. of the increase in  $F/F_0$ . The difference between nimodipine and control were significant ( $^* P < 0.05$ ) ( $n = 7$ ) (B).

- [3] Miller, R.L. and Vogt, R. (1996) An N-terminal partial sequence of the 13 kDa *Pycnopodia helianthoides* sperm chemoattractant 'startrak' possesses sperm-attracting activity. *J. Exp. Biol.* 199, 311–318.
- [4] Vacquier, V.D. and Moy, G.W. (1997) The fucose sulfate polymer of egg jelly binds to sperm REJ and is the inducer of the sea urchin sperm acrosome reaction. *Dev. Biol.* 192, 125–135.
- [5] Hansbrough, J.R. and Garbers, D.L. (1981) Speract. Purification and characterization of a peptide associated with eggs that activates spermatozoa. *J. Biol. Chem.* 256, 1447–1452.
- [6] Suzuki, N. (1995) Structure, function and biosynthesis of sperm-activating peptides and fucose sulfate glycoconjugate in the extracellular coat of sea urchin eggs. *Zool. Sci.* 12, 13–27.
- [7] Nishigaki, T. et al. (2004) A sea urchin egg jelly peptide induces a cGMP-mediated decrease in sperm intracellular  $\text{Ca}^{2+}$  before its increase. *Dev. Biol.* 272, 376–388.
- [8] Cook, S.P. and Babcock, D.F. (1993) Activation of  $\text{Ca}^{2+}$  permeability by cAMP is coordinated through the pH<sub>i</sub> increase induced by speract. *J. Biol. Chem.* 268, 22408–22413.
- [9] Reynaud, E., De de La Torre, L., Zapata, O., Lievano, A. and Darszon, A. (1993) Ionic bases of the membrane potential and intracellular pH changes induced by speract in swollen sea urchin sperm. *FEBS Lett.* 329, 210–214.
- [10] Kaupp, U.B. et al. (2003) The signal flow and motor response controlling chemotaxis of sea urchin sperm. *Nat. Cell Biol.* 5, 109–117.
- [11] Wood, C.D., Darszon, A. and Whitaker, M. (2003) Speract induces calcium oscillations in the sperm tail. *J. Cell. Biol.* 161, 89–101.
- [12] Solzin, J., Helbig, A., Van, Q., Brown, J.E., Hildebrand, E., Weyand, I. and Kaupp, U.B. (2004) Revisiting the role of  $\text{H}^{+}$  in chemotactic signaling of sperm. *J. Gen. Physiol.* 124, 115–124.
- [13] Vacquier, V.D. (1998) Evolution of gamete recognition proteins. *Science* 281, 1995–1998.
- [14] Schackmann, R.W., Eddy, E.M. and Shapiro, B.M. (1978) The acrosome reaction of *Strongylocentrotus purpuratus* sperm. Ion requirements and movements. *Dev. Biol.* 65, 483–495.
- [15] Gonzalez-Martinez, M.T., Galindo, B.E., de De La Torre, L., Zapata, O., Rodriguez, E., Florman, H.M. and Darszon, A. (2001) A sustained increase in intracellular  $\text{Ca}^{2+}$  is required for the acrosome reaction in sea urchin sperm. *Dev. Biol.* 236, 220–229.
- [16] Darszon, A., Nishigaki, T., Wood, C., Trevino, C.L., Felix, R. and Beltran, C. (2005) Calcium channels and  $\text{Ca}^{2+}$  fluctuations in sperm physiology. *Int. Rev. Cytol.* 243, 79–172.
- [17] Schackmann, R.W. (1989) in: *The Cell Biology of Fertilization* (Schatte, H. and Schatten, G., Eds.), pp. 3–28, Academic Press, San Diego.
- [18] Gauss, R., Seifert, R. and Kaupp, U.B. (1998) Molecular identification of a hyperpolarization-activated channel in sea urchin sperm. *Nature* 393, 583–587.
- [19] Galindo, B.E., Neill, A.T. and Vacquier, V.D. (2005) A new hyperpolarization-activated, cyclic nucleotide-gated channel from sea urchin sperm flagella. *Biochem. Biophys. Res. Commun.* 334, 96–101.
- [20] Catterall, W.A. (2000) Structure and regulation of voltage-gated  $\text{Ca}^{2+}$  channels. *Annu. Rev. Cell Dev. Biol.* 16, 521–555.
- [21] Catterall, W.A., Striessnig, J., Snutch, T.P. and Perez-Reyes, E. (2003) International Union of Pharmacology. XL. Compendium of voltage-gated ion channels: calcium channels. *Pharmacol. Rev.* 55, 579–581.
- [22] Arikath, J. and Campbell, K.P. (2003) Auxiliary subunits: essential components of the voltage-gated calcium channel complex. *Curr. Opin. Neurobiol.* 13, 298–307.
- [23] Okamura, Y., Izumi-Nakaseko, H., Nakajo, K., Ohtsuka, Y. and Ebihara, T. (2003) The ascidian dihydropyridine-resistant calcium channel as the prototype of chordate L-type calcium channel. *Neurosignals* 12, 142–158.
- [24] Jeziorski, M.C., Greenberg, R.M. and Anderson, P.A. (2000) The molecular biology of invertebrate voltage-gated  $\text{Ca}^{2+}$  channels. *J. Exp. Biol.* 203, 841–856.
- [25] Kumar, S., Tamura, K. and Nei, M. (2004) MEGA3: Integrated software for molecular evolutionary genetics analysis and sequence alignment. *Brief Bioinform.* 5, 150–163.
- [26] Garcia-Soto, J., Mourelle, M., Vargas, I., de De la Torre, L., Ramirez, E., Lopez-Colome, A.M. and Darszon, A. (1988) Sea urchin sperm head plasma membranes: characteristics and egg jelly induced  $\text{Ca}^{2+}$  and  $\text{Na}^{+}$  uptake. *Biochim. Biophys. Acta* 944, 1–12.
- [27] Rodriguez, E. and Darszon, A. (2003) Intracellular sodium changes during the speract response and the acrosome reaction in sea urchin sperm. *J. Physiol.* 546, 89–100.
- [28] González-Martínez, M., Guerrero, A., Morales, E., de De La Torre, L. and Darszon, A. (1992) A depolarization can trigger  $\text{Ca}^{2+}$  uptake and the acrosome reaction when preceded by a hyperpolarization in *L. pictus* sperm. *Dev. Biol.* 150, 193–202.
- [29] Garcia-Soto, J. and Darszon, A. (1985) High pH-induced acrosome reaction and  $\text{Ca}^{2+}$  uptake in sea urchin sperm suspended in  $\text{Na}^{+}$ -free seawater. *Dev. Biol.* 110, 338–345.
- [30] Wood, C.D., Nishigaki, T., Furuta, T., Baba, S.A. and Darszon, A. (2005) Real-time analysis of the role of  $\text{Ca}^{2+}$  in flagellar movement and motility in single sea urchin sperm. *J. Cell. Biol.* 169, 725–731.
- [31] Goodwin, L.O., Leeds, N.B., Hurley, I., Cooper, G.W., Pergolizzi, R.G. and Benoff, S. (1998) Alternative splicing of exons in the alpha1 subunit of the rat testis L-type voltage-dependent calcium channel generates germ line-specific dihydropyridine binding sites. *Mol. Hum. Reprod.* 4, 215–226.
- [32] Westenbroek, R.E. and Babcock, D.F. (1999) Discrete regional distributions suggest diverse functional roles of calcium channel alpha1 subunits in sperm. *Dev. Biol.* 207, 457–469.
- [33] Serrano, C.J., Trevino, C.L., Felix, R. and Darszon, A. (1999) Voltage-dependent  $\text{Ca}^{2+}$  channel subunit expression and immunolocalization in mouse spermatogenic cells and sperm. *FEBS Lett.* 462, 171–176.
- [34] Park, J.Y., Ahn, H.J., Gu, J.G., Lee, K.H., Kim, J.S., Kang, H.W. and Lee, J.H. (2003) Molecular identification of  $\text{Ca}^{2+}$  channels in human sperm. *Exp. Mol. Med.* 35, 285–292.
- [35] Trevino, C.L. et al. (2004) Expression and differential cell distribution of low-threshold  $\text{Ca}^{2+}$  channels in mammalian male germ cells and sperm. *FEBS Lett.* 563, 87–92.
- [36] Heinemann, S.H., Schlieff, T., Mori, Y. and Imoto, K. (1994) Molecular pore structure of voltage-gated sodium and calcium channels. *Braz. J. Med. Biol. Res.* 27, 2781–2802.
- [37] Wennemuth, G., Westenbroek, R.E., Xu, T., Hille, B. and Babcock, D.F. (2000)  $\text{CaV}2.2$  and  $\text{CaV}2.3$  (N- and R-type)  $\text{Ca}^{2+}$  channels in depolarization-evoked entry of  $\text{Ca}^{2+}$  into mouse sperm. *J. Biol. Chem.* 275, 21210–21217.